nature genetics

Evidence that homologous X-chromosome pairing requires transcription and Ctcf protein

Na Xu[1,3], Mary E Donohoe[1,3], Susana S Silva[1,2] & Jeannie T Lee[1]

X-chromosome inactivation (XCI) ensures the equality of X-chromosome dosages in male and female mammals by silencing one X in the female[1]. To achieve the mutually exclusive designation of active X (Xa) and inactive X (Xi), the process necessitates that two Xs communicate in *trans* through homologous pairing[2,3]. Pairing depends on a 15-kb region within the genes *Tsix* and *Xite*[2]. Here, we dissect molecular requirements and find that pairing can be recapitulated by 1- to 2-kb subfragments of *Tsix* or *Xite* with little sequence similarity. However, a common denominator among them is the presence of the protein Ctcf, a chromatin insulator[4–7] that we find to be essential for pairing. By contrast, the Ctcf-interacting partner, Yy1 (ref. 8), is not required. Pairing also depends on transcription. Transcriptional inhibition prevents new pair formation but does not perturb existing pairs. The kinetics suggest a pairing half-life of <1 h. We propose that pairing requires Ctcf binding and co-transcriptional activity of *Tsix* and *Xite*.

In the mouse, the X-inactivation center (*Xic*) orchestrates XCI through three noncoding genes: *Xite*[9], *Tsix*[10–12] and *Xist*[13–15]. *Xite* and *Tsix* designate the future Xa and are expressed on both Xs before XCI, whereas *Xist* initiates silencing and is expressed only from the Xi. The *Xic* works both in *trans* and in *cis*. In *trans*, *Xite* and *Tsix* coordinate the 'counting' of X chromosomes[16,17] and the mutually exclusive designation of Xa and Xi[18]. Once committed to XCI, *Xite* and *Tsix* become *cis* acting[9,19–21]: on the future Xa, their persistent expression blocks the upregulation of *Xist*[10,11], whereas on the future Xi, their repression induces *Xist* expression, which in turn initiates silencing of the linked X chromosome[13–15]. Although pairing is a prerequisite for the X-chromosome binary switch, the molecular underpinnings of this process have yet to be elucidated. Previous work has shown that a 3.7-kb fragment of *Tsix* (p3.7, **Fig. 1a**) and a 5.6-kb fragment of *Xite* (pXite) can recapitulate pairing in a transgene-based assay[2]. In mouse embryonic stem cells, the autosomal transgenes induce *de novo* pairing between the X and the autosome (X-A pairing) and prevent the formation of true X-X pairs[2], which in turn causes a failure of XCI[16].

To pinpoint specific *cis*- and *trans*-factor requirements, we created six small transgenes carrying specific motifs within *Tsix* or *Xite* (**Fig. 1a** and **Supplementary Table 1** online): pNS41 spans a 2.4-kb conserved region of *Tsix*[10] and several Ctcf-Yy1 elements[8]; pNS25 is a 1.6-kb fragment that contains *DXPas34*[17,22] and multiple Ctcf-Yy1

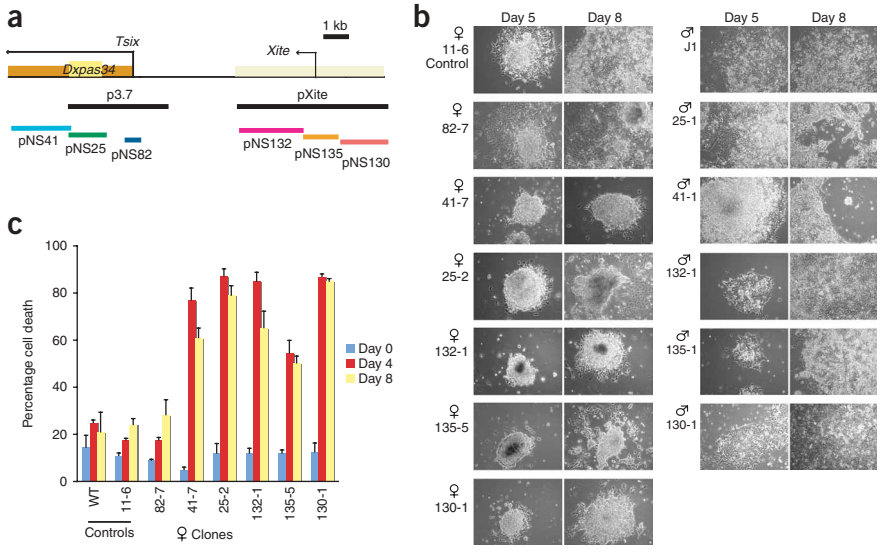

Figure 1 Growth and differentiation characteristics of new transgenic cell lines. (**a**) Map of *Tsix* and *Xite*, the previously characterized p3.7 and pXite transgenes and the six new transgenes. (**b**) Morphology and growth of embryoid bodies on day 5 and day 8 of differentiation. (**c**) Magnitude of cell death on day 0, day 4 and day 8 of differentiation. The averages of three independent experiments are shown. Error bars, s.d.

[1]Howard Hughes Medical Institute Department of Molecular Biology, Massachusetts General Hospital Department of Genetics, Harvard Medical School Boston, Massachusetts 02114, USA. [2]Gulbenkian PhD Programme in Biomedicine, Rua da Quinta Grande, 6, 2780-156, Oeiras, Portugal. [3]These authors contributed equally to this work. Correspondence should be addressed to J.T.L. (lee@molbio.mgh.harvard.edu).

Received 26 June; accepted 15 August; published online 21 October 2007; doi:10.1038/ng.2007.5

sites[8]; pNS82 contains the 0.22-kb minimal *Tsix* promoter[23] and a truncated Ctcf-Yy1 site; pNS132 spans a 2.5-kb *Xite* fragment with minor promoters and DNase I hypersensitive sites[9]; pNS135 consists of the 1.2-kb enhancer required for persistent *Tsix* expression on the future Xa[9,23]; pNS130 encompasses a 1.8-kb region upstream of the enhancer; and pNS11 (not shown) is a control containing only the vector. For each construct, we examined multiple clones. In all experiments that follow, three independent tests for each clone yielded similar results regardless of transgene copy number, so a representative clone for each transgene is shown.

All wild-type and transgenic female cell lines grew normally in the undifferentiated state (day 0, data not shown). However, upon differentiation into embryoid bodies to induce XCI, cell lines carrying pNS41 (for example, clone 41-7), pNS25 (for example, 25-2), pNS132 (for example, 132-1), pNS135 (for example, 135-5) and pNS130 (for

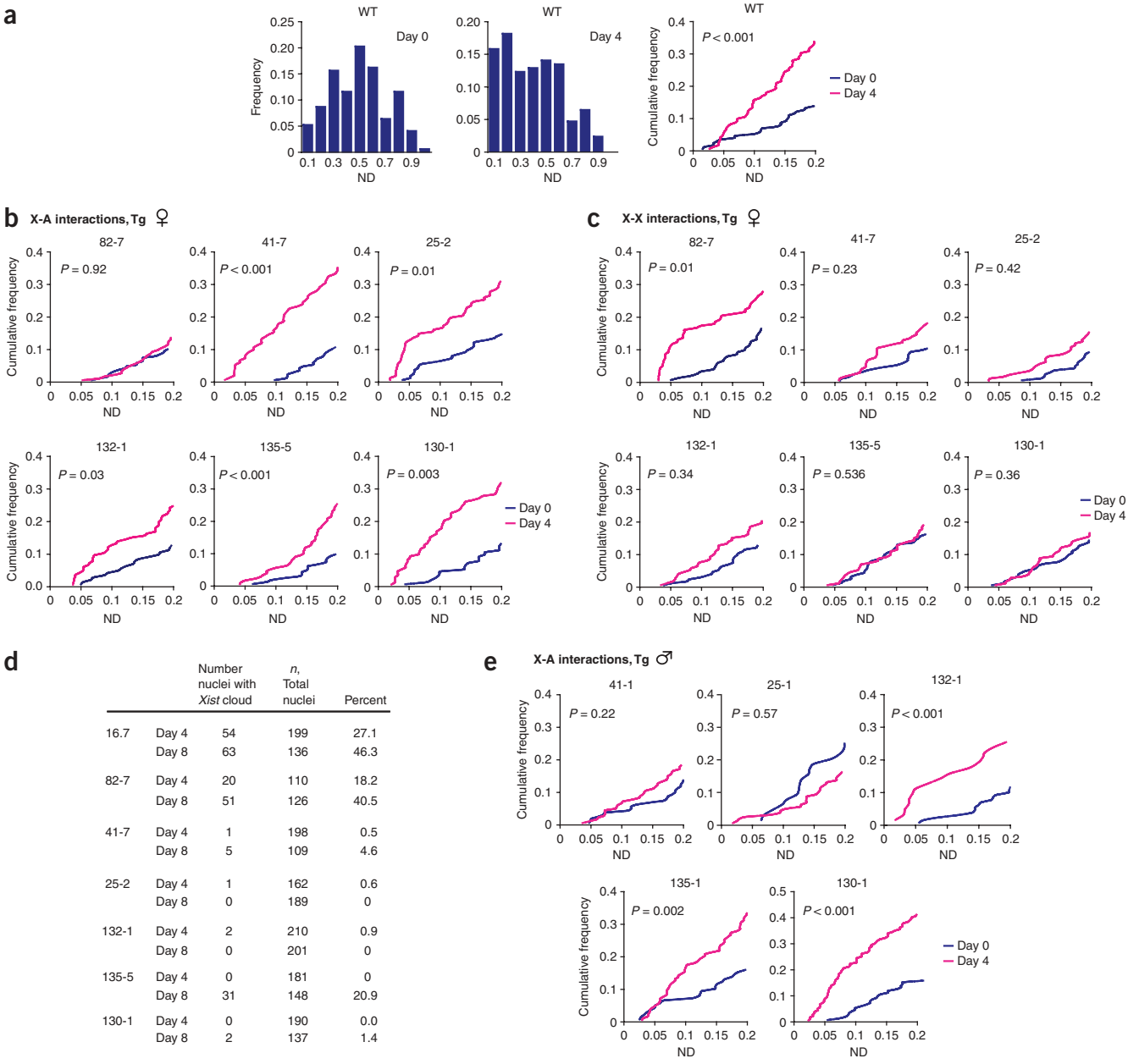

d

		Number nuclei with *Xist* cloud	*n*, Total nuclei	Percent
16.7	Day 4	54	199	27.1
	Day 8	63	136	46.3
82-7	Day 4	20	110	18.2
	Day 8	51	126	40.5
41-7	Day 4	1	198	0.5
	Day 8	5	109	4.6
25-2	Day 4	1	162	0.6
	Day 8	0	189	0
132-1	Day 4	2	210	0.9
	Day 8	0	201	0
135-5	Day 4	0	181	0
	Day 8	31	148	20.9
130-1	Day 4	0	190	0.0
	Day 8	2	137	1.4

Figure 2 Induction of ectopic X-A pairing, disruption of endogenous X-X pairing and compromised *Xist* upregulation. (**a**) Distribution of X-X distances in wild-type female embryonic stem cells on day 0 (left) and day 4 (middle). Cumulative frequencies at a normalized distance (ND) of 0.0–0.2 are shown at right. $n = 171$–173 nuclei counted. Normalized distance = *Xic-Xic* distance/d, where $d = 2 \times (\text{nuclear area}/\pi)^{0.5}$. Normalized distance ranges from 0 to 1. The significance of the difference between day 0 and day 4 (P) was determined by the Kolmogorov-Smirnov (KS) test, a nonparametric test to examine the null hypothesis that two independent datasets have the same distribution (SPSS 12.0 software). (**b**) Cumulative frequency curves for X-A distances in day 0 and day 4 transgenic female lines. $n = 151$–189. (**c**) Cumulative frequency curves for X-X distances for the cell populations in **b**. $n = 163$–193. (**d**) Frequency of *Xist* upregulation in day 4 and day 8 control and transgenic embryoid bodies, as determined by RNA FISH. (**e**) Cumulative frequency curves for X-A interactions in male transgenic lines. $n = 151$–189.

example, 130-1) all grew poorly (**Fig. 1b**), with elevated cell death between day 4 and day 8 (**Fig. 1c**). By contrast, wild-type embryoid bodies and vector-only embryoid bodies (for example, 11-6) differentiated normally. Embryoid bodies carrying the minimal *Tsix* promoter (for example, 82-7) also behaved normally. The effects were sex specific, as growth retardation and high cell death were seen in female but not male embryonic stem cells (**Fig. 1c** and data not shown). This is consistent with the sex-specific manifestation of *Tsix* and *Xite* defects on embryonic stem cell differentiation observed previously[9,11,16].

To determine whether the anomalies could be related to pairing defects, we followed chromosomal movements over time using FISH. As shown previously[2,3], the two Xs were randomly distributed relative to each other in the pre-XCI state (day 0) but became closely associated or 'paired' between day 2 and day 4 (that is, a normalized distance of <0.1), as shown by a left shift in X-X distance

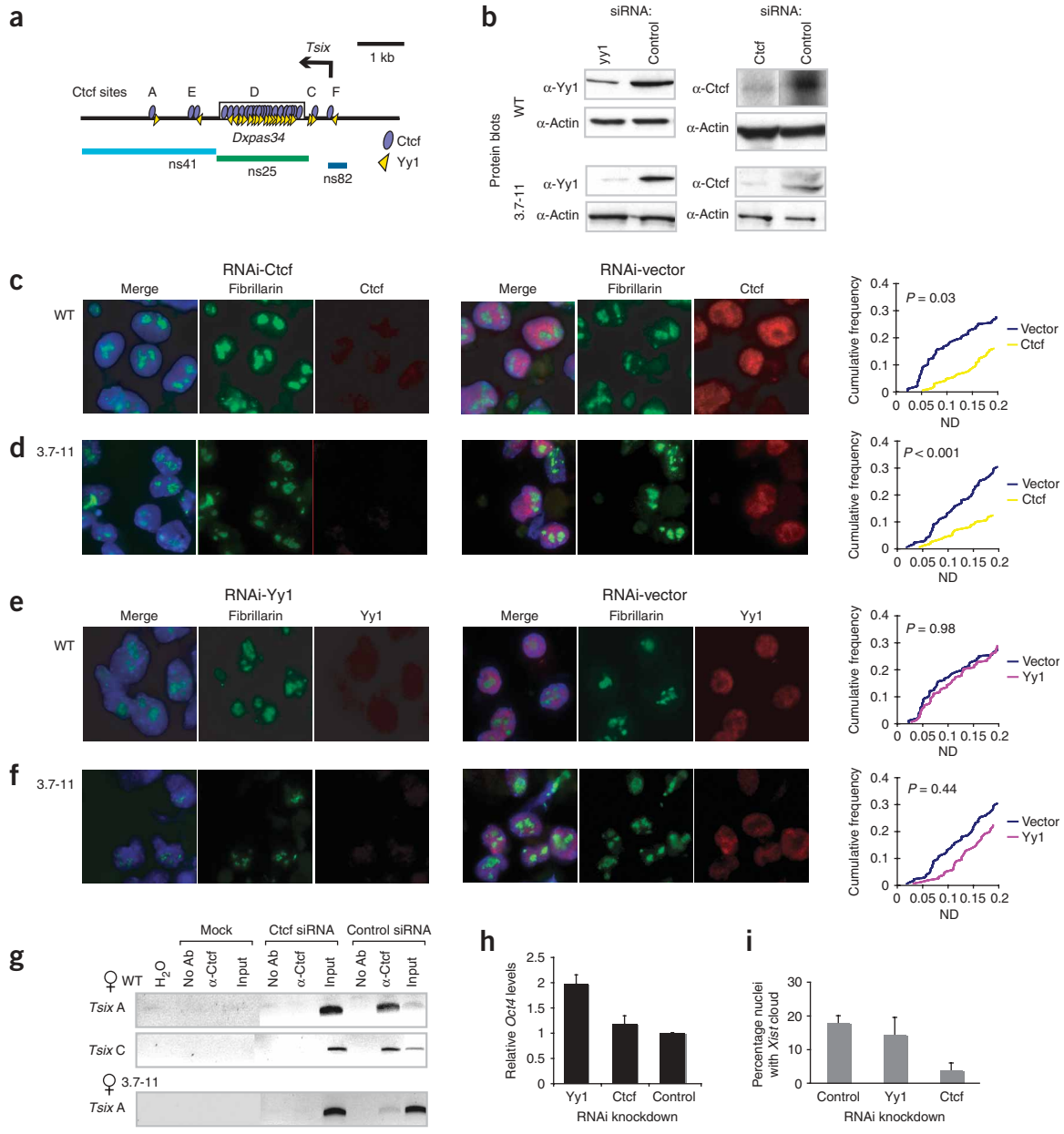

Figure 3 Ctcf protein is essential for pairing at *Tsix*. (**a**) Paired Ctcf-Yy1 elements at the 5′ end of *Tsix*. (**b**) Protein-blot analysis of Yy1 and Ctcf protein in the knockdown cells. Actin is used as loading control. α, antibody. (**c**,**d**) RNAi knockdown of Ctcf protein (red) in wild-type (WT) female embryonic stem cells (**c**) and transgenic 3.7-11 female cells (**d**). DAPI staining outlines the nuclear morphology (blue); immunostaining of fibrillarin (green) suggests unperturbed overall nuclear architecture. Cumulative frequency curves are shown for control (vector) and Ctcf knockdowns. We repeated all experiments at least three times. $n = 153$–181 nuclei counted per experiment. (**e**,**f**) RNAi knockdown of Yy1 protein (red). Experiments are as outlined in **c** and **d**. (**g**) ChIP using anti-Ctcf at *Tsix* in wild-type and transgenic 3.7-11 day 4 knockdown embryoid bodies. (**h**) Quantification of *Oct4* mRNA by real-time RT-PCR in the Yy1, Ctcf and control knockdowns shown in **c** and **e**. Each is normalized to β-actin. Primers and PCR as described[30]. (**i**) Frequency of *Xist* upregulation in Ctcf, Yy1 and control knockdown wild-type female cells. Averages of three experiments are shown. Error bars, s.d. $n > 100$ nuclei per experiment.

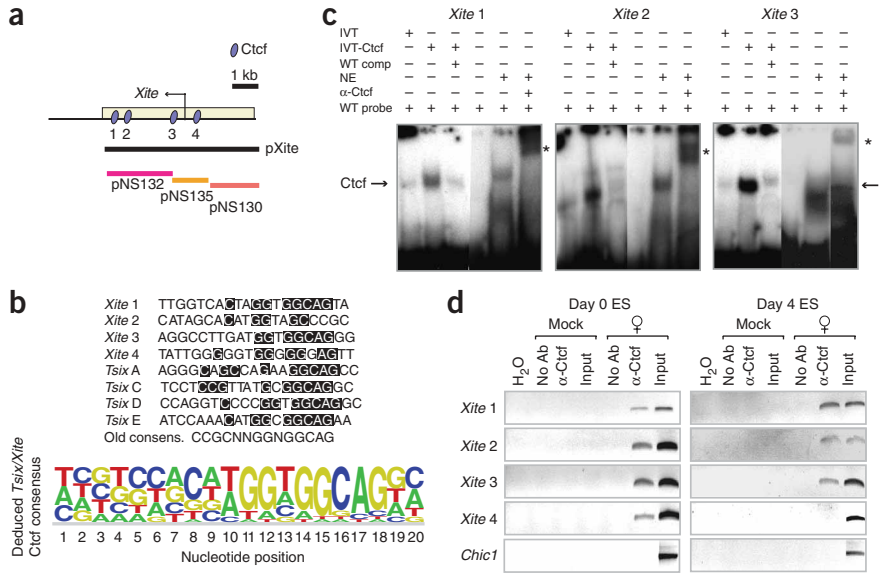

Figure 4 New Ctcf sites in *Xite*. (**a**) Map depicting the *Xite* locus, associated transgenes and new Ctcf sites. (**b**) Ctcf elements within *Tsix* and *Xite* as compared to the old Ctcf consensus, 5′-CCGCNNGGNGGCAG-3′. A newly deduced *Xic* Ctcf 20-bp consensus is shown below; the relative size of each nucleotide indicates the base's probability of occurrence at each position. (**c**) By EMSA, *in vitro*–translated Ctcf (IVT-Ctcf) or day 0 embryonic stem cell nuclear extract (NE) shifts labeled *Xite* 1, *Xite* 2 or *Xite* 3 oligos. Unprogrammed lysate produces a faint shift, possibly reflecting endogenous binding activity. Comp, cold competitors at 100× molar excess; WT, wild-type probe; arrow, Ctcf-DNA shift; asterisks, anti-Ctcf supershift; α, antibody. (**d**) ChIP analysis using anti-Ctcf in day 0 and day 4 wild-type female embryonic stem cells is shown for four *Xite* elements and the control *Chic1* locus. Mock, control immunoprecipitation with no chromatin added.

distributions relative to day 0 (**Fig. 2a**). In transgenic cells, the Xs and *Xic*-bearing autosomes were likewise randomly distributed on day 0, but they became closely associated on day 4 as the number of nuclei showing normalized X-autosome (X-A) distances of <0.1 increased (**Fig. 2b**). The only exception was 82-7, the cell line with normal growth and cell death (**Fig. 1b**).

To determine whether ectopic X-A interactions disrupted X-X interactions, we tracked X-X distances in the same cells (**Fig. 2c**). Indeed, the frequency of X-X pairing was markedly reduced in all transgenic lines except 82-7. The reduced pairing frequency correlated with decreased initiation of XCI, as measured by reduced formation of Xist RNA 'clouds' (**Fig. 2d**). Thus, *de novo* X-A association blocked formation of X-X pairs and inhibited XCI in female cells.

Among male lines, only the *Xite* subfragments, pNS132, pNS135 and pNS130, induced *de novo* X-A pairing (**Fig. 2e**), consistent with the previous observation that pXite, but not p3.7, could nucleate X-A pairing in males[2]. The data show that the *Xite* sequence is more effective at nucleating pairing than *Tsix*, as even a 1.2-kb *Xite* transgene induces pairing, whereas 5- to 15-kb *Tsix* transgenes do not[2]. However, in contrast to that in females, X-A pairing had no apparent physiologic consequence in males (**Fig. 1b**), further underscoring differences in the XX-versus-XY response to changes in *Tsix* and *Xite* dosage[2,16] in a manner consistent with a two-factor model for counting and choice[16,11,18].

These data indicated that pairing can be recapitulated by fragments as small as 1.2 kb with little to no obvious sequence similarity. However, we noted that several fragments contained the recently described Ctcf-Yy1 motifs[8] (**Fig. 3a**). Both Ctcf and Yy1 have multiple zinc fingers that can be used combinatorially to achieve functional diversity in their roles as transcription factor and chromatin insulator. Ctcf has also been implicated in long-range chromosomal interactions[24,25]. To test for a role of Ctcf-Yy1 in pairing, we depleted Ctcf or Yy1 by RNAi knockdown in day 2 female embryoid bodies and harvested on day 4 for analysis. Protein blotting (**Fig. 3b**) and immunofluorescence (**Fig. 3c–f**) confirmed protein depletion. Fibrillarin (nucleolar) staining and 4,6-diamidino-2-phenylindole (DAPI) staining suggested no gross disturbance to nuclear architecture (**Fig. 3c–f**).

By contrast, DNA FISH indicated a profound effect on pairing. In wild-type embryoid bodies, Ctcf knockdown reduced the frequency of X-X pairing to background levels (Compare **Fig. 3c** to day 0 data in

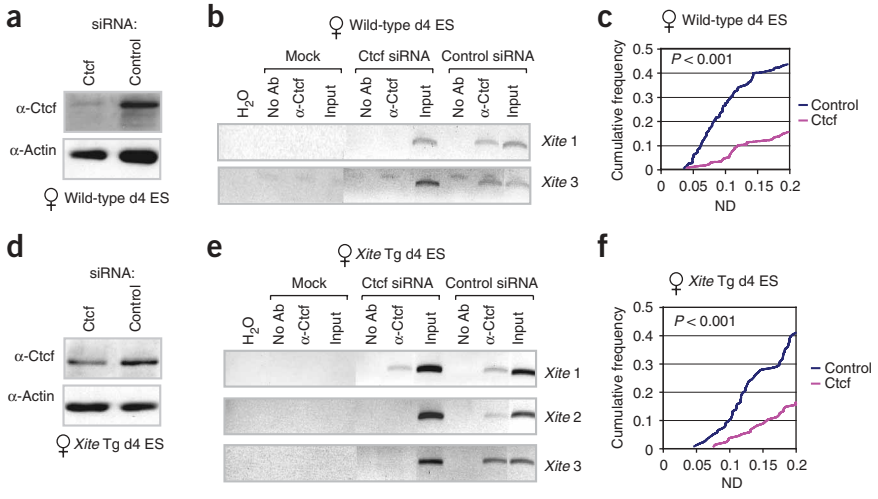

Figure 5 Ctcf protein is also required for pairing at *Xite*. (**a**) Protein-blot analysis of Ctcf and actin in knockdown and control female embryoid bodies (wild type) on day 4 of differentiation. (**b**) ChIP analysis of Ctcf binding at *Xite* and *Tsix* in knockdown and control cells corresponding to **a**. (**c**) Cumulative pairing frequency curves for Ctcf knockdown and control in wild-type female embryoid bodies. $n = 255$–277. (**d**) Protein-blot analysis of Ctcf and actin in knockdown and control Xite-11 transgenic embryoid bodies on day 4 of differentiation. (**e**) ChIP analysis of Ctcf binding in knockdown and control cells corresponding to **d.** (**f**) Cumulative pairing frequency curves for Ctcf knockdown and control in Xite-11 transgenic embryoid bodies. $n = 122$–135.

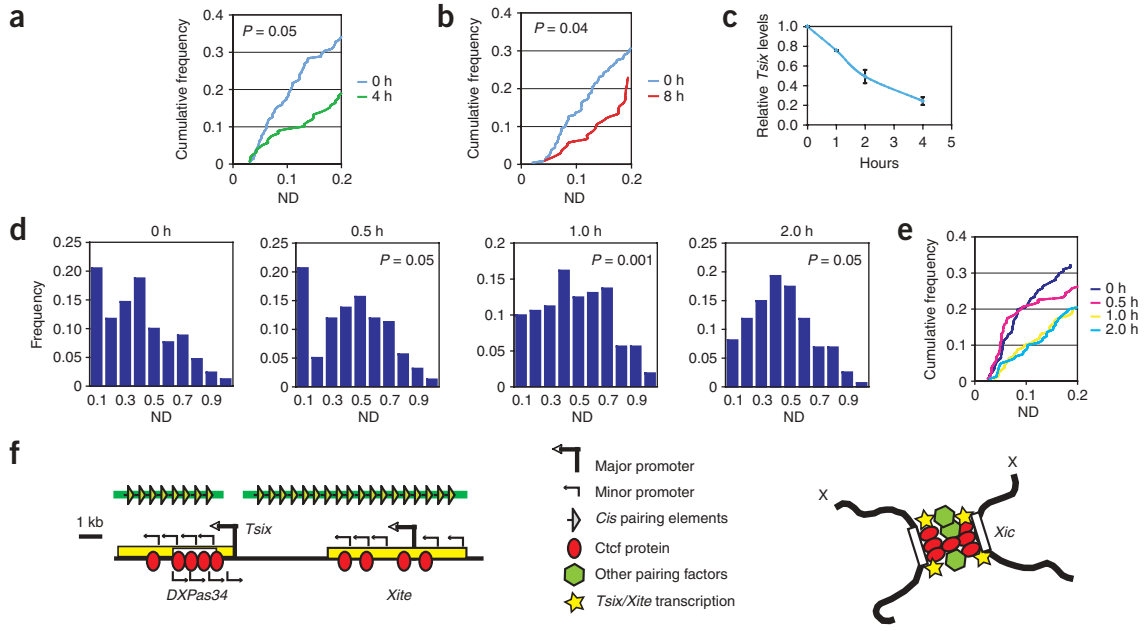

Figure 6 Analysis of transcription requirements. (**a**) Cumulative X-X pairing frequencies in day 2 wild-type female embryoid body cells treated with 5 μg/ml actinomycin D for 0 or 4 h. $n = 159–208$. (**b**) Cumulative X-X pairing frequencies in day 2 wild-type female embryoid body cells treated with 10 μg/ml α-amanitin for 8 h. $n = 105–222$. (**c**) Quantitative real-time, strand-specific RT-PCR of *Tsix* RNA confirmed that actinomycin D (shown) and α-amanitin (not shown) treatment disrupted Pol II activity. RNA levels are normalized to that of the 18S rRNA. Averages from three experiments. Error bars, s.d. (**d**) X-X distance distribution profiles in day 2 wild-type female embryoid body cells after 0, 0.5, 1.0 or 2.0 h of actinomycin D treatment. Kolmogorov-Smirnov test (*P*) compares each time point with the 0-h untreated sample. $n = 160–171$. (**e**) Cumulative frequency curves of the distributions shown in **d**. (**f**) Summary of *cis* and *trans* factors for pairing at *Tsix* and *Xite*. Left, the critical pairing region and functionally redundant pairing elements therein (light green triangles). Ctcf sites are found throughout *Tsix* and *Xite*. Ctcf cannot be working alone, as pNS130 appears to lack binding sites but still nucleates pairing. Other pairing proteins (hexagons) are likely to exist. Transcriptional activity is also required (note that multiple minor and cryptic promoter elements can be found throughout the region). Right, a working model in which X-X pairing is held together by Ctcf proteins and transcriptional activity or RNA at *Tsix* and *Xite*.

Fig. 2a). In 3.7-11 transgenic embryoid bodies, Ctcf knockdown likewise disrupted interchromosomal pairing (**Fig. 3d**). Chromatin immunoprecipitation (ChIP) using antibody to Ctcf (anti-Ctcf) indicated that Ctcf binding at *Tsix* was indeed reduced (**Fig. 3g**). Notably, depleting the interacting partner, Yy1, did not affect pairing in either case (**Fig. 3e**,**f**). These results suggested that the effect of Ctcf is specific and is not a consequence of altered cell differentiation rate, as downregulation of the Oct4 pluripotency factor occurred normally (**Fig. 3h**); nor is it the consequence of decreased cell viability, as the number of heteropyknotic cells determined by Hoechst 33258 staining[26] was ≪5% in both Ctcf-knockdown and control-knockdown cells (**Supplementary Fig. 1** online). Measurements were taken only in the nonapoptotic fraction. The Ctcf knockdown concurrently disrupted formation of *Xist* clouds (**Fig. 3i**), consistent with the idea that the initiation of XCI depends on X-X pairing[2,3]. We conclude that Ctcf is a *trans*-acting mediator of X-X pairing at the *Tsix* locus.

Although Ctcf sites have been mapped within *Tsix*, they had not been described in *Xite*. Given that small *Xite* transgenes could also mediate pairing (**Fig. 2**), we next investigated whether Ctcf also binds *Xite*. Bioinformatic analysis using established Ctcf consensus motifs[4,5–7,27] revealed four potential sites within the tested fragments (**Fig. 4a**,**b**; note that pNS130 may contain sites that elude detection by the Ctcf algorithm, which identifies only a fraction of *in vivo* sites[27]). Electrophoretic mobility shift assays (EMSA) showed that *in vitro* synthesized Ctcf protein gel-shifted ^{32}P-labeled *Xite* sites, which were competed away by unlabeled *Xite* oligonucleotides (**Fig. 4c** and data not shown). Unprogrammed lysates produced only a faint shift (endogenous activity). Incubation with nuclear extract from the embryonic stem cells resulted in a DNA-protein complex that supershifted when exposed to anti-Ctcf (**Fig. 4c**). Furthermore, ChIP showed that Ctcf binds all four *Xite* elements in pre-XCI female embryonic stem cells (day 0). On day 4, Ctcf binds all but *Xite* 4 (**Fig. 4d**). We conclude that, like *Tsix*, *Xite* complexes with Ctcf both *in vitro* and *in vivo*. We deduced a 20-bp Ctcf consensus for the *Xic* (**Fig. 4b**) using established methods[27,28].

To determine whether Ctcf also mediates pairing at *Xite*, we knocked down Ctcf in wild-type female embryoid bodies on day 2 and harvested cells for analysis on day 4. Protein analysis indicated that Ctcf protein was considerably depleted (**Fig. 5a**); ChIP analysis confirmed that Ctcf binding at *Xite* was consequently disrupted (**Fig. 5b**). Examination of interchromosomal distances revealed that Ctcf depletion did markedly reduce X-X pairing (**Fig. 5c**). We observed a similar effect on X-A pairing in the Xite-11 (ref. 16) transgenic line when Ctcf was knocked down and Ctcf binding was at least partially disrupted at *Xite* (**Fig. 5d–f**; note that residual binding may reflect residual Ctcf activity, as shown by protein-blot analysis). Thus, we propose that Ctcf mediates interchromosomal pairing at both *Tsix* and *Xite*, either by directly bridging two chromosomes or indirectly through other factors. The occurrence of Ctcf-binding sites is therefore one notable common denominator among disparate pairing-competent transgenes.

Another common thread among the transgenes is their potential to drive transcription, as cryptic promoters have been shown to exist outside of the primary *Tsix* and *Xite* initiation sites—all of which are

DNA polymerase II (Pol II) directed[9,12,21–23]. To determine whether transcriptional activity is required for pairing, we treated wild-type embryoid bodies (day 2) with either actinomycin D for 4 h (**Fig. 6a**) or α-amanitin for 8 h (**Fig. 6b**) and confirmed Pol II inhibition by measuring a drop in *Tsix* transcription (**Fig. 6c**). Notably, Pol II inhibition resulted in a consistent disruption of X-X pairing.

To establish the kinetics of pairing loss, we treated day 2 wild-type female embryoid bodies with actinomycin D for 0, 0.5, 1.0 and 2.0 h (**Fig. 6d**). At 2 h and beyond, the X-X distribution profiles differed significantly from those at the 0-h time point ($P = 0.05$) and resembled the random distribution typical of pre-XCI cells (compare **Fig. 6d**, 2-h time point, and **Fig. 2a**, day 0), indicating that pairing persists for less than 2 h in the absence of new transcription. At the 1-h time point, the distribution was intermediate, with fewer pairs in the 0.0–0.2 normalized-distance range than at the 0-h time point ($P = 0.001$, **Fig. 6d**), indicating that pairs begin to disintegrate after ~1 h. Notably, at 0.5 h, the profile was bimodal: whereas the 0.2–1.0 normalized-distance profile suggested a random distribution, the number of pairs separated by a normalized distance <0.1 remained unchanged (**Fig. 6d**,**e**). Three independent experiments yielded similar results at all time points. Thus, inhibition of transcription immediately abolished the formation of new X-X pairs but did not disrupt pre-existing pairs. These results suggested that nucleation of X-X pairing requires new transcription or its associated RNA, but the maintenance of existing pairs does not.

Conveniently, the sensitivity of new pair formation to transcriptional inhibitors enabled us to estimate the half-life ($t_{1/2}$) of X-X pairs. Because more than 50% of the X-X pairs with a separation of normalized distance <0.1 were lost after 1 h of actinomycin D treatment (**Fig. 6d**), the half-life must be <1.0 h. This range is consistent with the observations that X-X pairing occurs very transiently[2,3] and that an X-X separation of normalized distance <0.1 can be observed in fewer than 15–20% of any day 2–4 embryoid body population (**Fig. 2a**).

In conclusion, our analysis has revealed new *cis* and *trans* requirements for homologous chromosome pairing. Within the 15-kb critical domain for counting, choice and pairing[16], fragments as small as 1–2 kb—each with overtly different primary sequences—can promote pair formation, at least when multimerized on a transgene array. We have identified Ctcf sites as a common motif among them and shown that the Ctcf protein mediates interchromosomal pairing. Although we cannot exclude indirect and general effects of Ctcf on pairing, the abundance of Ctcf motifs in *Tsix* and *Xite* indicates that at least some effects must be locus specific. Ctcf could directly mediate pairing (**Fig. 6f**) or collaborate with additional factors. Given Ctcf's ubiquitous nature, it seems likely that additional factors must be involved in regulation. Indeed, pairing may occur co-transcriptionally with *Tsix* and *Xite*, as new transcription is required to create new pairs. Together with Ctcf protein, *Tsix* and *Xite* RNAs may form an 'RNA-protein bridge' between two Xs (**Fig. 6f**). Once formed, such an RNA-protein bridge might have transient stability, accounting for the apparent insensitivity of existing pairs to transcriptional inhibitors during the first half-hour of treatment. With other epigenetic phenomena being subject to intra- and interchromosomal regulation[24,25,29], the properties described here for homologous chromosome pairing are likely to be relevant for many other mammalian loci.

METHODS

Embryonic stem cell lines, transgenesis and culture. Wild-type male J1 (40XY) and female 16.7 (40XX) embryonic stem cell lines and transgenic lines 3.7-11 and Xite-11 have all been previously described[11,16]. We created new transgenic lines by linearizing 30–40 μg of plasmids (**Supplementary Table 1**; plasmids as described in ref. 23), electroporating the DNA into 10^7 16.7 or J1 cells at 240 V and 500 μF using the Bio-Rad Genepulser, and selecting for clones in 300 μg/ml G418 for 7–9 days. We analyzed at least three independent clones for each construct (each with similar results). All clones were maintained under G418 selection. Differentiation was induced by EB suspension culture and withdrawal of LIF. On day 4, we attached embryoid bodies to gelatinized plates to promote outgrowth of differentiated cells. We carried out analysis of cell death using the trypan blue method as described[16].

FISH. Embryonic stem cells were trypsinized into single cells, cytospun on glass slides and fixed in 4% paraformaldehyde/1× PBS. We then carried out FISH as described[2,10]. We labeled probes with fluorescein-12-dUTP, Cy3-dUTP or AlexaFluor-555-dUTP by nick translation (Roche). We used probes pSxN and pSx9 for general detection of the *Xic*, a *neo* probe for specific detection of the transgene locus[2] and a single-stranded riboprobe cocktail for detection of the *Xist* RNA[23]. For analysis of pairing, we took digital images with the Zeiss AxioPlan2 and processed them using OpenLab software (Improvision; see details in ref. 2). In brief, *z* sections were captured at 0.2 μ intervals and three-dimensional images were projected on a single two-dimensional plane. We measured *Xic-Xic* distances (x) and the nuclear areas (A) using the OpenLab software. Only nuclei with two resolvable X signals were scored (single dots were excluded). 'Normalized distance' (ND) is defined as x/d, where d is the nuclear diameter, defined as $2(A/\pi)^{0.5}$.

Transgene copy number analysis. We estimated transgene copy number by quantitative FISH. For each clone, we carried out FISH using a probe corresponding to the *Xic* transgene fragment and determined the total intensity in arbitrary units (S) using Openlab software, which integrates the intensities of all the pixels in the signal area. The transgene signal (S_{tg}) was distinguished from the endogenous *Xic* signal (S_x) by colocalization to a *neo* probe. We determined the transgene copy number as S_{tg}/S_x and classified it as low (2–5 copies), medium (6–10 copies) or high (>10 copies).

RNAi knockdown. We carried out siRNA-mediated knockdowns of Ctcf and Yy1 proteins using mouse Ctcf SMARTpool siRNA and *yy1* BS/U6 Pol III vectors, respectively, as described[8]. We used vector-only or *gfp* siRNAs in control knockdowns. In brief, small hairpin RNA (shRNA; 4 μg) or short interfering RNAs (siRNAs; 0.8 μM) were delivered into day 2 wild-type or transgenic female embryoid bodies using the Amaxa Biosystems Nucleofector/Mouse ES Nucleofector Kit. Day 4 embryoid bodies were harvested 46–48 h later. Ctcf and Yy1 knockdowns were confirmed by protein-blot analysis using rabbit anti-Ctcf (Upstate), mouse anti-Yy1 (Santa Cruz H10) and mouse anti–β-actin (Chemicon), with the appropriate rabbit or mouse secondary antibodies conjugated to horseradish peroxidase for detection (Western Lightening Chemiluminescence Kit; Perkin Elmer Life Sciences). Immunostaining was carried out using anti-fibrillarin (Abcam 38F3), anti-Yy1 and anti-Ctcf, with detection using secondary Alexa555-goat anti-rabbit or Alexa488 anti-mouse (Molecular Probes).

EMSA. We carried out EMSAs using 20 fmol of oligonucleotides with 1–2 μg undifferentiated embryonic stem cell nuclear extract or 1 μl *in vitro*–translated Ctcf (TNT-coupled reticulocyte system, Promega)[4]. Cold competitors were added at 100× molar excess. See **Supplementary Table 2** online for oligo sequences. Supershifts were carried out with 2 μl of anti-Ctcf (Upstate).

ChIP. ChIP, antibodies, real-time PCR, and *Tsix* and *Chic1* PCR primers have been described[8]. *Xite* primer sequences are shown in **Supplementary Table 2**. For ChIP on knockdown samples, we harvested 3×10^6–10×10^6 cells nucleofected cells on day 4 to perform ChIP.

Transcription inhibition. Three independent biological replicates yielded similar results. Day 2 wild-type female embryoid bodies were treated with 5 μg/ml actinomycin D or 10 μg/ml α-amanitin as described[21,22]. Embryoid bodies were then harvested at 0, 0.5, 1.0, 2.0, 4.0 and 6.0 h and subjected to FISH or quantitative RT-PCR analysis. For real-time RT-PCR, we isolated RNAs using Trizol, treated 1 μg of total RNA with RNase-free DNase, reverse transcribed the RNA using random primers, and amplified 200 ng of cDNA

using the Bio-Rad iCycler iQ real-time PCR detection system in SYBRGreen. All samples were normalized to the 18S rRNA internal control in Pol II inhibition experiments[22]. *Tsix* RT-PCR was used to confirm Pol II inhibition using primers as described[8].

Note: Supplementary information is available on the Nature Genetics website.

ACKNOWLEDGMENTS

We thank all members of the Lee laboratory for stimulating discussion and feedback throughout this work. S.S.S. is partially funded by a doctoral fellowship from the Gulbenkian Institute–Portugal (Fundacao para a Ciencia e a Tecnologia SFRH/BD/9614/2002). This work was supported by an US National Institutes of Health grant (RO1-GM58839) to J.T.L., who is an investigator of the Howard Hughes Medical Institute.

AUTHOR CONTRIBUTIONS

N.X., M.E.D. and J.T.L. designed this study; N.X. created and analyzed transgenes and performed pairing, RNA FISH, immunofluorescence and transcription analyses; M.E.D. performed knockdowns, western blot, ChIP, EMSA, bioinformatics and qRT-PCR analyses; S.S. contributed to pairing analyses; J.T.L. wrote the paper and supervised the research.

Published online at http://www.nature.com/naturegenetics
Reprints and permissions information is available online at http://npg.nature.com/reprintsandpermissions

1. Lyon, M.F. Gene action in the X-chromosome of the mouse (*Mus musculus* L.). *Nature* **190**, 372–373 (1961).
2. Xu, N., Tsai, C.L. & Lee, J.T. Transient homologous chromosome pairing marks the onset of X inactivation. *Science* **311**, 1149–1152 (2006).
3. Bacher, C.P. *et al.* Transient colocalization of X-inactivation centres accompanies the initiation of X inactivation. *Nat. Cell Biol.* **8**, 293–299 (2006).
4. Chao, W., Huynh, K.D., Spencer, R.J., Davidow, L.S. & Lee, J.T. CTCF, a candidate trans-acting factor for X-inactivation choice. *Science* **295**, 345–347 (2002).
5. Bell, A. & Felsenfeld, G. Methylation of a CTCF-dependent boundary controls imprinted expression of the *Igf2* gene. *Nature* **405**, 482–485 (2000).
6. Hark, A.T. *et al.* CTCF mediates methylation-sensitive enhancer-blocking activity at the H19/Igf2 locus. *Nature* **405**, 486–489 (2000).
7. Kanduri, C. *et al.* Functional association of CTCF with the insulator upstream of the H19 gene is parent of origin-specific and methylation-sensitive. *Curr. Biol.* **10**, 853–856 (2000).
8. Donohoe, M.E., Zhang, L., Xu, N., Shi, Y. & Lee, J.T. Identification of a CTCF co-factor, YY1, for the X-chromosome binary switch. *Mol. Cell* **25**, 43–56 (2007).
9. Ogawa, Y. & Lee, J.T. Xite, X-inactivation intergenic transcription elements that regulate the probability of choice. *Mol. Cell* **11**, 731–743 (2003).
10. Lee, J.T., Davidow, L.S. & Warshawsky, D. Tsix, a gene antisense to Xist at the X-inactivation centre. *Nat. Genet.* **21**, 400–404 (1999).
11. Lee, J.T. & Lu, N. Targeted mutagenesis of Tsix leads to nonrandom X inactivation. *Cell* **99**, 47–57 (1999).
12. Sado, T., Wang, Z., Sasaki, H. & Li, E. Regulation of imprinted X-chromosome inactivation in mice by Tsix. *Development* **128**, 1275–1286 (2001).
13. Brockdorff, N. *et al.* The product of the mouse Xist gene is a 15 kb inactive X-specific transcript containing no conserved ORF and located in the nucleus. *Cell* **71**, 515–526 (1992).
14. Brown, C.J. *et al.* The human XIST gene: analysis of a 17 kb inactive X-specific RNA that contains conserved repeats and is highly localized within the nucleus. *Cell* **71**, 527–542 (1992).
15. Wutz, A., Rasmussen, T.P. & Jaenisch, R. Chromosomal silencing and localization are mediated by different domains of Xist RNA. *Nat. Genet.* **30**, 167–174 (2002).
16. Lee, J.T. Regulation of X-chromosome counting by Tsix and Xite sequences. *Science* **309**, 768–771 (2005).
17. Vigneau, S., Augui, S., Navarro, P., Avner, P. & Clerc, P. An essential role for the DXPas34 tandem repeat and Tsix transcription in the counting process of X chromosome inactivation. *Proc. Natl. Acad. Sci. USA* **103**, 7390–7395 (2006).
18. Lee, J.T. Homozygous Tsix mutant mice reveal a sex-ratio distortion and revert to random X-inactivation. *Nat. Genet.* **32**, 195–200 (2002).
19. Navarro, P., Pichard, S., Ciaudo, C., Avner, P. & Rougeulle, C. Tsix transcription across the Xist gene alters chromatin conformation without affecting Xist transcription: implications for X-chromosome inactivation. *Genes Dev.* **19**, 1474–1484 (2005).
20. Sado, T., Hoki, Y. & Sasaki, H. Tsix silences Xist through modification of chromatin structure. *Dev. Cell* **9**, 159–165 (2005).
21. Sun, B.K., Deaton, A.M. & Lee, J.T. A transient heterochromatic state in Xist preempts X inactivation choice without RNA stabilization. *Mol. Cell* **21**, 617–628 (2006).
22. Cohen, D.E. *et al.* The Dxpas34 repeat regulates random and imprinted X-inactivation. *Dev. Cell* **12**, 57–71 (2007).
23. Stavropoulos, N., Rowntree, R.K. & Lee, J.T. Identification of developmentally specific enhancers for Tsix in the regulation of X chromosome inactivation. *Mol. Cell. Biol.* **25**, 2757–2769 (2005).
24. Kurukuti, S. *et al.* CTCF binding at the H19 imprinting control region mediates maternally inherited higher-order chromatin conformation to restrict enhancer access to Igf2. *Proc. Natl. Acad. Sci. USA* **103**, 10684–10689 (2006).
25. Ling, J.Q. *et al.* CTCF mediates interchromosomal colocalization between Igf2/H19 and Wsb1/Nf1. *Science* **312**, 269–272 (2006).
26. Syken, J., De-Medina, T. & Munger, K. TID1, a human homolog of the *Drosophila* tumor suppressor l(2)tid, encodes two mitochondrial modulators of apoptosis with opposing functions. *Proc. Natl. Acad. Sci. USA* **96**, 8499–8504 (1999).
27. Kim, T.H. *et al.* Analysis of the vertebrate insulator protein CTCF-binding sites in the human genome. *Cell* **128**, 1231–1245 (2007).
28. Workman, C.T. *et al.* enoLOGOS: a versatile web tool for energy normalized sequence logos. *Nucleic Acids Res.* **33**, W389–92 (2005).
29. Spilianakis, C.G., Lalioti, M.D., Town, T., Lee, G.R. & Flavell, R.A. Interchromosomal associations between alternatively expressed loci. *Nature* **435**, 637–645 (2005).
30. Nichols, J. *et al.* Formation of pluripotent stem cells in the mammalian embryo depends on the POU transcription factor Oct4. *Cell* **95**, 379–391 (1998).